Nano Research
2023, 16(4): 5817–5825

ISSN 1998-0124 CN 11-5974/O4
https://doi.org/10.1007/s12274-022-5165-x

Research Article

Revisiting the single-step synthesis of quantum dots: The hidden ligand-promoted surface reaction channels

Qiyu Yu[1,2] (✉), Jiaxin Song[3], Ke Li[1,2], and Lili Xiao[1,2]

[1] College of Materials Science and Engineering, Sichuan University of Science and Engineering, Zigong 643000, China
[2] Key Laboratory of Material Corrosion and Protection of Sichuan Province, Zigong 643000, China
[3] College of Physics, Sichuan University, Chengdu 610065, China

Received: 1 September 2022 / **Revised:** 30 September 2022 / **Accepted:** 3 October 2022

ABSTRACT

In this work, we revisited the single-step synthesis of CdE (E = S, Se, and Te) quantum dots (QDs). Powdered CdO and elemental chalcogen were directly used for heating-up synthesis. Firstly, the *in situ* dissolution of the solid precursors and related QD formation channels were preliminarily investigated. In general, QDs were generated from homogeneous reactions between dissolved cadmium and chalcogen precursors in bulk solution. We found that, during single-step synthesis, both the dissolution of CdO and selenium proceeded faster than their *ex situ* dissolution respectively. To explain this result, we proposed the existence of extra surface reaction channels for QD formation. That is, QDs could also be generated via on-surface reactions between the solid precursors and the dissolved counter precursors (as "ligands"). The happening of these extra surface reactions would increase the overall dissolution rate of CdO and selenium. Further, the circulation of oleic acid which is peculiar to such single-step synthesis should also partly account for the accelerated dissolution of CdO. Finally, by comparing with two-step synthesis using pre-dissolved CdO, we presented that such single-step synthesis was reliable in making uniform CdE QDs with good reproducibility. Our work reaffirmed the great potential of this single-step strategy in cost-effective synthesis of monodisperse QDs. Moreover, the ligand-promoted surface reaction channels would be applicable in solution-phase synthesis of metal chalcogenide nanocrystals from solid precursors.

KEYWORDS

quantum dots, reaction channel, surface reaction, single-step synthesis, heating-up synthesis

1 Introduction

Colloidal semiconductor quantum dots (QDs) have great potential in optical and optoelectronic applications [1–5]. The solution-phase synthesis of QDs achieved great progress in the past three decades [1, 2, 6]. In the pioneering work in 1993, Bawendi and coworkers detailed the synthesis of CdE (E = S, Se, and Te) QDs via a hot-injection route, where organometallic precursors such as dimethyl cadmium and phosphine chalcogenide were rapidly injected into a hot coordinating solvent, tri-n-octylphosphine oxide (TOPO) [7]. One of the most important insights of this work was to restrict nucleation to an initial burst (achieved by hot-injection in their work), which was key to generating high-quality QDs with a low size dispersion [2, 7]. Based on this hot-injection organometallic route, the synthesis of QDs, presented by CdE QDs, has been extensively studied. On one hand, greener synthetic chemistries were introduced, enabling facile and environmentally benign synthesis. The replacement of organometallic cadmium precursors by CdO made cheaper and safer lab synthesis possible [8]. The substitution of non-coordinating solvent, e.g., 1-octadecene (ODE) for TOPO, combined with the introduction of surface-capping ligands such as oleic acid (OA) and alkylphosphonic acid, also brings in environmentally friendlier, yet more controllable synthesis [9, 10]. The phosphine-free synthesis of QDs also represents a great attempt toward greener synthesis [11, 12]. On the other hand, heating-up (also known as noninjection) techniques were pursued to achieve facile, up-scalable yet high-quality synthesis [13–16]. Cao and coworkers brought in the concept that nucleation can be tightly controlled by carefully choosing precursors, reaction parameters, additional initiators, etc. By doing these, heating-up synthesis can produce high-quality QDs comparable to the best ones prepared by hot-injection methods. Despite the achievements, current synthesis of QDs is not yet mature, and studies on synthetic mechanisms have significantly lagged behind. The molecular mechanisms taking place in bulk solution [17–21] and QD surfaces [22, 23] can hardly be accessible. Besides, the investigation of the reaction channels pertaining to nucleation and growth of QDs is also a grand challenge [24–29]. Lacking knowledge of these mechanisms hampers attempts to control related processes thermodynamically and kinetically for rational QD synthesis.

Previously reported works by Zhang et al. [30–32] inspired our study. Pre-dissolution of CdO and elemental chalcogen are routinely adopted preparatory steps in the injection-based or heating-up synthesis of CdE QDs. Particularly, one may take it for granted that CdO should be dissolved to make a homogenous cadmium precursor solution for the synthesis of CdE QDs. In their reports, however, Zhang et al. demonstrated that CdS, CdSe, and related core–shell QDs could be effectively prepared directly

Address correspondence to yuqiyu2008@163.com

from CdO and elemental chalcogen via a single-step heating-up method [30–32]. The preparatory steps of precursor solution making are not trivial, but even more time- and energy-consuming than QD synthesis itself. The dissolution of CdO in oleic acid or alkylphosphonic acid generally requires heating at temperatures of 200–300 °C [8–10, 12, 14]. The preparation of phosphine-free selenium stock solution (in ODE, liquid paraffin, etc.) also needs prolonged heating at around 200 °C, and may suffer from loss of toxic H_2Se gas [11, 12, 33]. Particularly, the dissolution of elemental tellurium in organophosphines, the mostly used way to a homogeneous tellurium precursor, is rather difficult. Long time heating in an excessive amount of organophosphine is generally needed for complete dissolution [34–36]. Efforts have been made to find alternatives to these precursors. Particularly, selenium powder or heterogeneous Se–ODE dispersions were found to be very convenient yet effective selenium precursors for the syntheses of CdSe QDs and other selenide nanocrystals [14, 37–39]. The direct use of both CdO and elemental chalcogens presented by Zhang et al. further simplified the synthetic operation and is amenable for large scale and inexpensive QD synthesis. Despite effectiveness, the direct use of CdO and chalcogen powders in liquid-phase synthesis will introduce additional processes of precursor dissolving *in situ*, which should exert influence on the synthesis of QDs. However, mechanisms concerning the dissolution of the solid precursors and the formation of the QDs thereof were not much discussed in their reports [30–32].

To make an effort to fulfil the potential of this single-step strategy, we revisited the single-step synthesis using CdO-derived plain CdE QDs as model systems, with an emphasis on the *in situ* dissolution of the solid precursors and their effects on synthesis. We demonstrate that the direct use of these solid precursors would not delay the QD synthetic progress, but can indeed make a difference to QD synthesis. From the perspective of reaction rate, we found that the dissolution of the solid precursors of CdO and selenium during synthesis was faster as compared with their *ex situ* dissolution respectively. To explain this result, we proposed extra ligand-promoted surface reaction channels for the dissolution of the solid precursors and the formation of QDs thereof. We further demonstrated that CdS QDs could be synthesized from solid CdO via a sole channel of ligand-promoted surface reaction. Particularly, we proposed that "OA circulation" during the single-step synthesis should at least partly account for the accelerated dissolution of CdO. Finally, by comparing with two-step syntheses using pre-dissolved CdO, we showed that monodisperse CdS and CdSe QDs could be prepared by using this single-step strategy. Our study reaffirmed the unique charm of the single-step heating-up strategy. And importantly, our study revealed hidden ligand-promoted surface reaction channels for QD formation, which should be useful in nanocrystal synthesis via nanoscale surface reactions.

2 Results and discussion

2.1 Co-dissolution of cadmium oxide and elemental chalcogens is different

In this work, we investigated the single-step synthesis of plain CdE QDs. Cationic and anionic precursors of CdO and chalcogen powders, in addition to all other reagents, were directly introduced into the reaction vessel at room temperature, and then heated up for corresponding QD synthesis. The recipes were adjusted from previous reports [9, 10, 12, 14]. CdO, selenium (sulfur), and OA were used for CdSe (CdS) synthesis. CdO, tellurium, OA or 1-tetradecylphosphonic acid (TDPA), and trioctylphosphine (TOP) were used for CdTe synthesis. ODE was used as the solvent in these syntheses. In the single-step syntheses, the solid–liquid reaction mixtures were directly heated to the setting temperatures for QD growth, without staying at a relatively low temperature for complete dissolution of CdO and elemental chalcogen [40]. As a result, the dissolution of these powdered starting materials was partly integrated into the QD growth process. Qualitatively, we explored the dissolution of the CdO and selenium during synthesis by comparing with their *ex situ* dissolution respectively (see Experimental), and found that the dissolution of both CdO and selenium during single-step synthesis was accelerated (Fig. 1).

2.1.1 *Accelerated in situ dissolution of cadmium oxide*

We found that the dissolution of CdO in the presence of sulfur was largely accelerated, as compared with the dissolution of CdO alone. The serial pictures in Figs. 1(a) and 1(b) give a presentation of CdO dissolution in the absence and presence of sulfur, respectively, upon heating at 200 °C within 30 min. The reason for the selection of a moderate temperature of 200 °C is such that the dissolution is neither too time-consuming nor too fast to observe the difference between the two cases. It appears that the CdO powder in the presence of sulfur largely disappeared within 10 min, while it took more than 30 min for the CdO to dissolve into a clear cadmium oleate solution in the absence of sulfur precursor. Presumably, the accelerated dissolution of CdO is partly attributed to "OA circulation" during single-step synthesis, as illustrated by Reactions (1) and (2)

$$\mathrm{CdO(s)} + \mathrm{HOA} \rightarrow \mathrm{Cd(OA)_2} \quad (1)$$

$$\mathrm{Cd(OA)_2} + \mathrm{S(sol)} \rightarrow \mathrm{CdS} + \mathrm{HOA} \quad (2)$$

The released OA during QD formation (Reaction (2)) will in turn promote the dissolution of CdO (Reaction (1)). Compared with the dissolution of CdO alone, a relatively higher concentration of OA can thus be maintained and drive faster dissolution of CdO. The release of carboxylic acid during QD formation has already been reported for phosphine-free and phosphine-based synthesis of QDs [18, 33, 41, 42].

A further comparison suggests that the acceleration effect of CdO dissolution was more obvious in the presence of sulfur than in the presence of selenium. In the presence of sulfur, as demonstrated in Fig. 1(b), the CdO powder largely dissolved at 200 °C/10 min. In the presence of selenium, however, quite a bit of CdO powder remained undissolved at the same stage (Fig. 1(c)). This difference should be related to the much more readily dissolution of sulfur powder than selenium in ODE. At 200 °C/10 min, sulfur had already dissolved completely, while selenium was largely undissolved. Therefore, the OA circulation at an early stage was faster in the presence of sulfur than in the presence of selenium.

2.1.2 *Accelerated in situ dissolution of elemental chalcogens*

The dissolution of selenium was also accelerated during the single-step synthesis of QDs. The serial pictures in Figs. 1(c) and 1(d) give a presentation of selenium dissolution in the presence and absence of CdO, respectively, upon heating at 200 °C within 30 min. Analogously, the *in situ* dissolution of selenium (Fig. 1(c)) was faster than its dissolution alone (Fig. 1(d)). At 20 min, significantly less undissolved selenium powders were observed in the presence of the cadmium precursor. At 30 min, a portion of selenium powders still remained undissolved in the absence of the cadmium precursor; while no obvious selenium powders were observed in the presence of the cadmium precursor.

The influence of the cadmium precursor was also verified in the

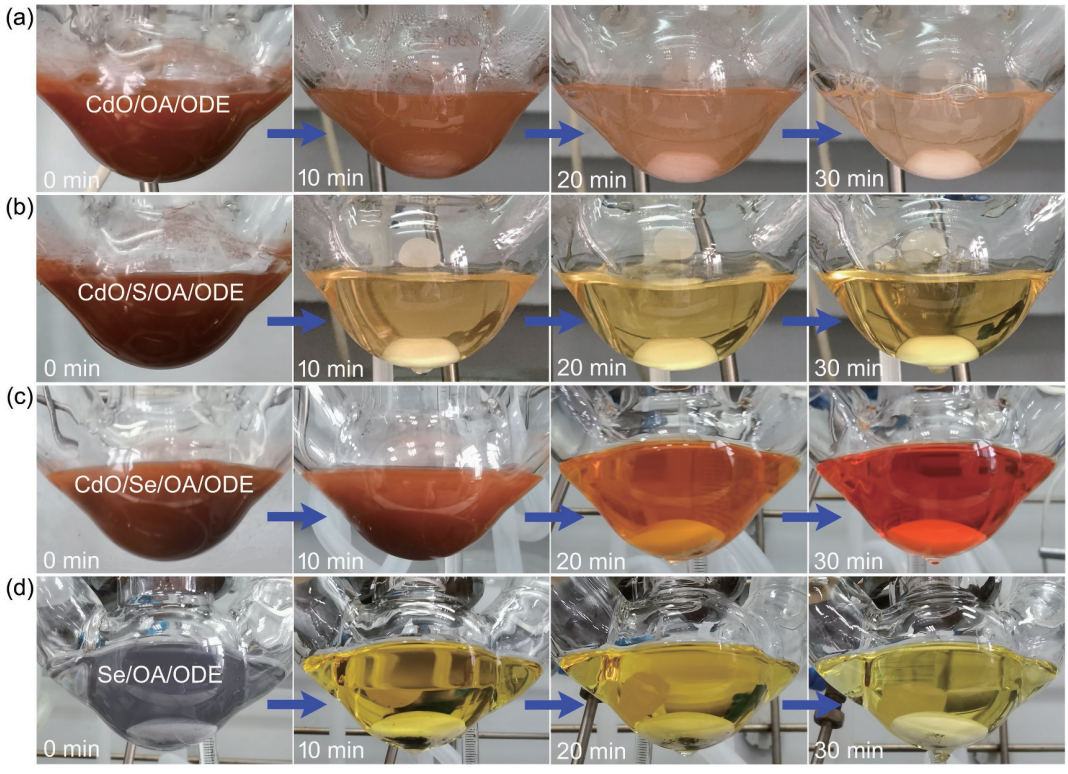

Figure 1 Digital pictures exhibiting the dissolution of CdO and selenium each respectively with and without counter precursors. Four mixtures of (a) CdO/OA/ODE, (b) CdO/S/OA/ODE, (c) CdO/Se/OA/ODE, and (d) Se/OA/ODE were heated at 200 °C. Pictures were taken at 0, 10, 20, and 30 min, respectively.

case of tellurium dissolution. During the synthesis of CdTe QDs, accelerated tellurium dissolution was also observed. Using TDPA as ligand, tellurium and CdO remained almost unchanged and no sign of CdTe generation was detected after heating at 220 °C for 30 min. However, if OA or myristic acid was used instead of TDPA, significant dissolution of tellurium and the generation of CdTe nanocrystals were already detected below 200 °C (Fig. S1 in the Electronic Supplementary Material (ESM)). In the latter case, the accelerated dissolution of tellurium should be related to the relatively easier dissolution of CdO into the bulk solution in the presence of the carboxylic acids than in the presence of TDPA [10]. The above results suggest that the presence of the dissolved cadmium precursors rather than solid CdO influenced the dissolution of selenium and tellurium. It should be pointed out that sulfur dissolution occurred quickly during the heating-up process, and thus was not affected by the presence of CdO.

2.2 Ligand-promoted surface reaction channels for QD formation

Under the present conditions, the dissolution of selenium in ODE occurs far from thermodynamic equilibria [43]. Therefore, the promotion of selenium dissolution via pulling the dissolution equilibria can be excluded. The acceleration of selenium dissolution implies that the dissolved cadmium precursor directly participated in and promoted the dissolution process. To explain the acceleration effect, we proposed the presence of an extra ligand-promoted surface reaction channel involved with the dissolved cadmium precursor, besides the direct dissolution of chalcogen into the bulk solution. In such a channel, the dissolved cadmium precursor initiated on-surface reactions with the chalcogen solid to form QDs (Fig. 2(a)). An analogous surface reaction channel might also be applicable for the dissolution of CdO (Fig. 2(b)). Taking the formation of CdSe QDs as an example, such channels of precursor dissolution and QD formation can be depicted in Fig. 2.

The proposed ligand-promoted surface reaction channels

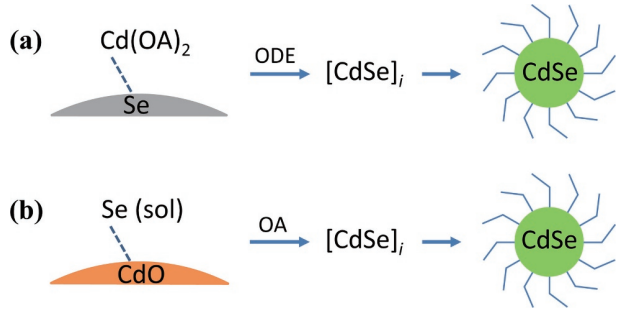

Figure 2 Schematic illustration of the formation of CdSe QDs via reactions on the surfaces of bulk (a) CdO and (b) selenium, respectively. The reactions took place on the surfaces of the solid, between (a) the cationic sites and the solubilized anionic precursor or (b) the reverse. The surface reactions supply $[CdSe]_i$ monomers to the bulk solution.

borrowed knowledge from mineral weathering [44–46]. The reaction channels illustrated in Fig. 2 can be simply described as follows. At first, the dissolved cationic and anionic precursors as "ligands" were adsorbed respectively on the undissolved selenium and CdO via surface complexation. Such complexation resembles the "half-reactions" on QD surfaces [22, 47]. Then, the complexed cadmium or selenium center was detached and displaced into the bulk solution to form $[CdSe]_i$ monomers [16, 21, 48]. Finally, the monomers nucleated to form CdSe QDs. OA complexation with the same cadmium center promoted its detachment from the CdO surface (Fig. 2(b)). ODE (for selenium) or phosphines (for tellurium) as the major reducing agent also participated in the surface reaction preceding the detachment (Fig. 2(a)) [45, 46]. Such surface reaction channels may also lead to OA circulation as the homogeneous QD formation channel in the bulk solution (Reaction (2)).

The proposed surface reaction mechanism in Fig. 2(b) can also explain the faster dissolution of CdO in the presence of sulfur than in the presence of selenium (Figs. 1(b) and 1(c)). First, the much easier dissolution of sulfur than selenium facilitates faster surface

complexation with CdO. Besides, the chemical affinity of the dissolved chalcogen toward CdO surface should also influence the surface complexation process. The reported bond dissociation energies of Cd–S and Cd–Se bonds are 208.5 ± 20.9 and 127.6 ± 25.1 kJ/mol, respectively [49], suggesting a stronger chemical affinity of sulfur than selenium toward CdO surface.

The feasibility of QD formation via the ligand-promoted surface channel was verified by further experiments. We carried out three experiments to support the proposed channels. In Experiment 1, oleyamine (OLA) was utilized to replace oleic acid in the single-step synthesis of CdS QDs. A CdO/S/OLA/ODE mixture was heated at 220 °C for 20 min, and then the undissolved CdO was removed and discarded. For comparison, we performed a similar experiment in two steps (Experiment 2). In the first step, a CdO/OLA/ODE mixture was heated at 220 °C for 20 min, and then the supernatant was isolated from undissolved CdO. In the second step, the decanted supernatant was mixed with sulfur, and heated to 220 °C for 20 min. For further comparison with Experiment 1, another control experiment was performed in the absence of OLA. See Experimental for more details. The optical properties of the resulting liquid phases in Experiments 1 and 2 (Fig. 3) indicate that CdS QDs were produced in the single-step method but not in the two-step method. In Experiment 3, no sign of CdS generation was detected in the liquid phase or in the undissolved solid phase (Fig. S2 in the ESM).

The reason for choosing OLA as ligand in Experiment 1 lies in that OLA cannot dissolve CdO as OA does. The result of Experiment 2 verified that CdO cannot dissolve into OLA under the present condition. Therefore, the formation of CdS QDs via homogeneous reactions between cationic and anionic precursors in the bulk solution can be excluded in Experiment 1. It is safe to decide that the generation of CdS QDs in Experiment 1 was initiated by heterogeneous on-surface reactions with CdO. The result of Experiment 3 further underlines the critical role of the OLA ligand in the surface reactions. In the absence of OLA, although sulfur easily dissolved in ODE and was reactive at the experimental temperature, the reaction could not take place. This is possibly because of high activation energies for the diffusion of atoms and ions in bulk CdO [50]. The results of Experiments 2 and 3 indicate that OLA or dissolved sulfur alone cannot solubilize CdO. Therefore, it is safe to conclude that OLA and dissolved sulfur as ligands have a synergistic effect on the dissolution of CdO in Experiment 1. Our results are reminiscent of previous findings that thiol–amine can dissolve bulk meal oxide including cadmium oxide [51, 52]. Likely, the dissolved sulfur in ODE in this work plays a similar role of thiols in those works. As a matter of fact, the synergistic effects of different ligands have been widely used in various applications [53, 54].

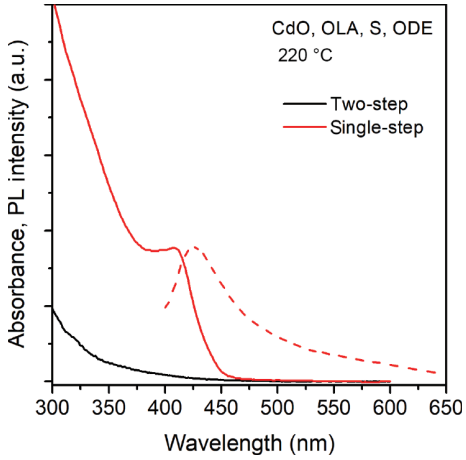

Figure 3 UV–vis absorption and PL spectra of samples prepared using CdO, sulfur, OLA, and ODE. In the single-step synthesis, a CdO/S/OLA/ODE mixture was directly heated up. In the two-step synthesis, a mixture of CdO, OLA, and ODE was heated first; then the supernatant was decanted, remixed with sulfur, and heated up.

In our experiments with the CdO/S/OLA/ODE mixtures, we found that the reactions were very slow and CdO could not dissolve completely. We estimate that the proposed QD formation channels illustrated in Fig. 2 also proceeded at a relatively slower rate, and the channel via Reaction (2) in bulk solution is dominant. It is easy to imagine higher reaction rates if nanoscale surfaces are involved. Our study on the formation channels of QDs is preliminary, and we could not give any quantitative information about the reaction channels involved in the single-step synthesis. We are doing further experiments to get to know more about these channels.

Noteworthily, CdO may function as an important intermediate in precursor conversion in some syntheses of QDs using preformed cadmium carboxylate [42, 55]. Therefore, we estimate that the surface reaction channel in Fig. 2(b) might also play a role even in those syntheses. The direct use of CdO for synthesis is not common so far; whereas, selenium powder and Se–ODE heterogeneous suspensions have been widely used for selenide QD synthesis [14, 37, 38]. We estimate that the proposed surface reaction channel in Fig. 2(a) might be involved in the selenium dissolution in those reported cases. For an amazing example, selenium was directly used for one-pot synthesis of magic-sized CdSe clusters at temperatures as low as 120 °C [56], despite the report that selenium can hardly dissolve in ODE below 150 °C [43]. We estimate that such synthesis should proceed, to a large extent, via heterogenous reactions between bulk selenium surfaces and the highly reactive cadmium precursor that readily formed from cadmium acetate and fatty acid.

2.3 Single-step synthesis of CdE QDs

We characterized the single-step synthesis of CdE (E = S, Se, and Te) QDs, as demonstrated in Fig. 4. For the synthesis of CdS QDs, CdO (0.5 mmol), sulfur (0.25 mmol), and OA (3.5 mmol) were mixed with ODE, heated up to 220 °C (ca. 10 °C/min), and kept at this temperature for 30 min for the growth of QDs. Analogously, CdSe QDs can be prepared by replacing sulfur with selenium (0.25 mmol). In the case of CdTe QD preparation, tellurium (0.25 mmol), TDPA (1.1 mmol), TOP (1.1 mmol), and ODE were heated to a higher temperature of 290 °C. See Experimental for more details.

The temporal evolution of ultraviolet–visible (UV–vis) absorption and photoluminescence (PL) spectra during synthesis suggest quite controllable growth of the CdE QDs (Fig. 4(a)). The growth of the QDs in size mainly occurs within the first 10–15 min of the temperature-keeping stage. CdS and CdSe samples exhibit clearly resolved absorption transitions in the absorption spectra and give narrow band gap PL emission peaks, with negligible trap emission. The optical property suggests that as-prepared CdS and CdSe QDs were fairly monodisperse. Reaction parameters, such as the temperature and the relative amount of capping ligand, can be modified without undermining the quality of the products (Fig. S3 in the ESM). Transmission electron microscopy (TEM) images (Fig. 4(b)) of as-prepared CdE QDs indicate uniform dot-shaped particles. After the heating-up synthesis for CdS and CdSe QDs, the premixed solid–liquid mixtures turned into clear colloidal dispersions, without undissolved solids remaining (Fig. S4 in the ESM). Powder X-ray diffraction (PXRD) patterns of the CdS and CdSe QDs also exhibit no sign of impurities from undissolved precursors (Fig. S5 in the ESM). The quality of the QD products can be further optimized

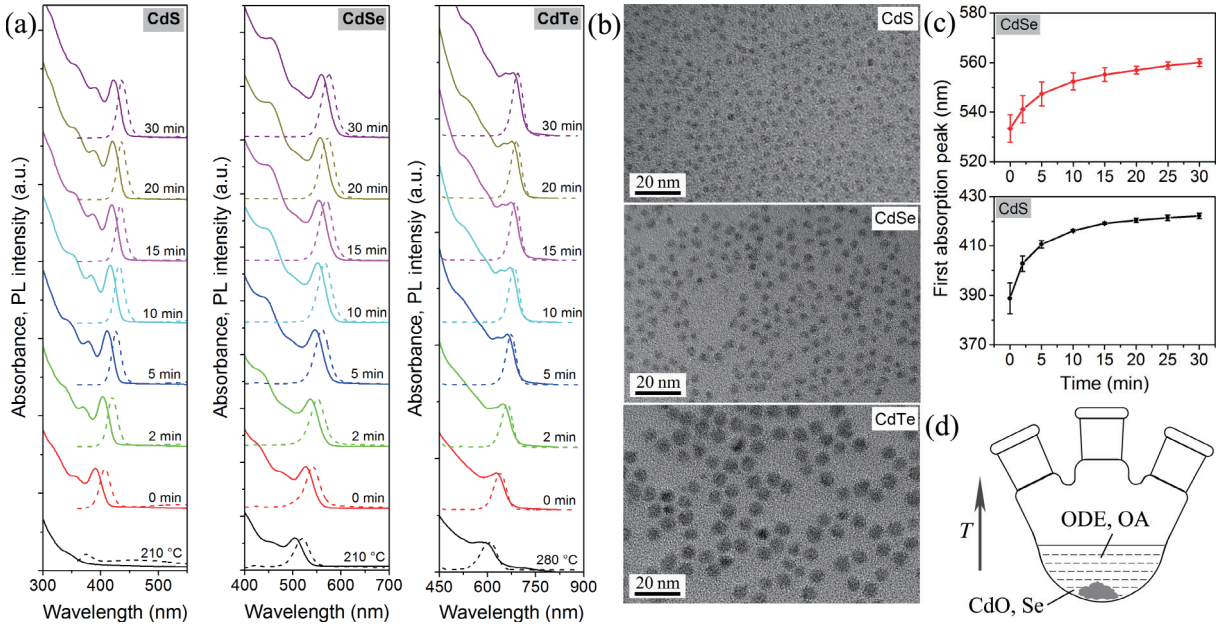

Figure 4 (a) UV–vis absorption (solid) and PL (dashed) spectra obtained during the growth of CdS, CdSe, and CdTe QDs. The setting temperature for QD growth was 220 °C for CdS and CdSe, and was 290 °C for CdTe. (b) Typical TEM images of the QDs. (c) Temporal evolution of the first absorption wavelengths of the CdS and CdSe QDs during synthesis. (d) A schematic illustration of the singe-step synthetic strategy, exemplified by the synthesis of CdSe QDs.

by carefully choosing acidic surfactant and reaction parameters.

The batch-to-batch consistency of the QD growth for this single-step strategy was examined. Figure 4(c) exhibits the temporal evolution of the first absorption maxima of CdS and CdSe QDs based on five parallel syntheses. During synthesis, the fluctuation in particle size appears in the initial rapid-growth stage, within about 15 min. This fluctuation may be arising from sampling time deviations and different dissolving rates of the powdered precursors. The discrepancy in particle size is largely compensated during the prolonged reaction. After 30 min of reaction, the syntheses give products with very similar first absorption wavelengths. This result indicates that the single-step synthesis, although starting from a heterogeneous mixture (Fig. 4(d)), is controllable and reproducible, and is applicable for large-scale synthesis of QDs with desired sizes.

CdO is a commonly used starting material for the synthesis of CdE nanocrystals. Prior to the direct use of CdO for heating-up synthesis by Zhang et al. [30–32], another cadmium source, cadmium acetate, had also been used in the heating-up synthesis of CdS QDs. In a report by Cao et al., cadmium acetate and sulfur were directly used in the heating-up synthesis of CdS QDs with the help of initiators [13]. It seems that cadmium acetate, more readily dissolved with an acidic or basic surfactant, should be an excellent cadmium source for single-step heating-up synthesis. But as it happens, cadmium acetate is much less used for QD synthesis than CdO. The main reason is the influence of acetate on nanocrystal growth [57, 58]. In the report of Cao et al., though not emphasized, prolonged vacuum degassing at about 120 °C was a must to remove the nascent acetic acid [13, 57, 59]. This vacuum procedure caused inconvenience and any presence of acetate in the reaction mixture may cause poor reproducibility of synthesis. Actually, cadmium acetate-based methods have been well known for the synthesis of magic size clusters or nanoplatelets rather than conventional QDs [48, 56, 60, 61].

2.4 Single-step synthesis vs. two-step synthesis

For comparison, we carried out two-step syntheses of CdS and CdSe QDs, where sulfur or selenium was directly used but CdO was routinely dissolved in advance. Under otherwise the same conditions, such experiments were done to explore the effect of *in situ* dissolution of CdO on the QD growth. See Experimental and Fig. S6 in the ESM for more details and results. The analyses of QD growth in typical single-step synthesis and the two-step synthesis are presented in Fig. 5. The size and size distribution can be judged by the location of first absorption and the full width at half-maximum (FWHM) of PL peak, respectively. The QD concentration was calculated using Peng's equations [62]. The CdS QDs prepared from the single-step approach generally have a smaller size and slightly higher particle concentration than those prepared with the two-step method (Figs. 5(a) and 5(b)). Moreover, the results also suggest that the *in situ* dissolution of the solid precursors would not delay the QD synthetic progress. The PL FWHM of the CdS QDs in singe-step synthesis decreased quickly at an early stage and then stabilized at ca. 19 nm, while the value gradually increased from 16 to 21 nm during the two-step synthesis (Fig. 5(c)). This result indicates that the single-step method can produce CdS QDs with roughly similar quality to the two-step method, but is more controllable in size dispersion. Similar but much more obvious tendencies were observed in the case of CdSe QDs. As demonstrated in Figs. 5(d)–5(f), the CdSe QDs prepared with the single-step method have substantially smaller sizes, higher concentrations, and narrower size dispersions than those prepared with the two-step method. The yield of CdSe QDs at an early stage of the two-step synthesis was higher than that of the single-step synthesis, and then the yields of the two synthetic methods tend to be similar at later stages (Fig. S7 in the ESM).

The intrinsic conversion kinetics of the precursors has a more profound effect on the nucleation and growth of QDs in the heating-up synthesis compared with that in the injection-based synthesis. Therefore, the judicious selection of precursors is of paramount importance for the heating-up synthesis of high-quality QDs [16]. The reason for the variation in growth kinetics and QD quality of the two methods originates from the different reactivity of CdO and the preformed cadmium oleate. Compared with solid CdO, solubilized cadmium oleate should be more reactive. In the two-step syntheses using cadmium oleate, monomers were formed rapidly, resulting in rapid nucleation and growth rates (Fig. S7 in the ESM). As soon as nucleation was triggered, the nuclei grew rapidly by absorbing the monomers

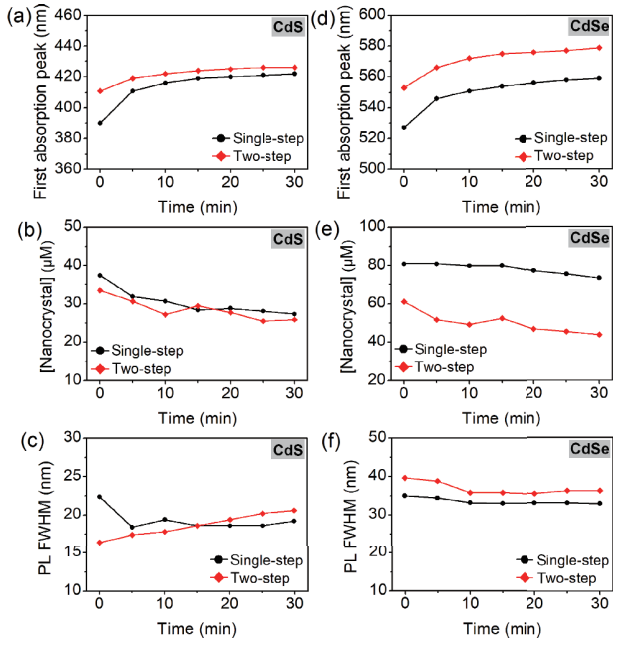

Figure 5 Comparison of typical single-step and two-step syntheses of CdS ((a)–(c)) and CdSe ((d)–(f)) QDs each respectively. Data were extracted from the temporal evolution of the absorption and PL spectra at 220 °C: ((a) and (d)) first absorption peak wavelengths, ((b) and (e)) nanocrystal concentrations, and ((c) and (f)) widths of PL peaks. The data of the two-step synthesis were extracted from the absorption spectra presented in Fig. S6 in the ESM.

quickly, which discontinued nucleation. Consequently, relatively low nanocrystal concentrations and big sizes were obtained [16]. The relationship between precursor reactivity and nanocrystal concentration was discussed in many reports. We noticed that our results are consistent with those observed in heating-up syntheses [13, 14], but are opposite to what was observed in the hot-injection syntheses [9, 63–65]. These conflicting results are surprising yet fascinating. In the hot-injection methods, nucleation was restricted to an initial burst. Therefore, the injection of a more reactive precursor would lead to a larger number of nuclei.

The results in Fig. 5 indicate that the direct use of CdO was able to produce QDs with narrower size dispersions than those prepared using preformed cadmium oleate. In the two-step heating-up synthesis of CdSe QDs, nucleation occurred at a relatively low temperature stage (around 170 °C) when selenium powder remained largely undissolved. In this case, the relatively large QD sizes with inhomogeneous distributions were caused by the imbalance between nucleation and growth. In other words, compared with preformed cadmium oleate, solid CdO has a better matched reactivity toward selenium powder [13, 14, 16]. In the case of CdS synthesis, however, sulfur already dissolved prior to nucleation (around 210 °C). In the single-step synthesis, the dissolution of solid CdO occurred quickly at this nucleation temperature, and therefore was able to result in uniform QDs like the two-step method.

3 Conclusions

By revisiting the single-step synthesis of QDs, our study provides some insights into the solution-phase synthesis of cadmium chalcogenides that directly utilizes CdO and/or selenium solid precursors:

(i) The dissolution of CdO and chalcogens (selenium and tellurium) during the single-step synthesis was accelerated, compared with their dissolution respectively alone.

(ii) Extra ligand-promoted surface reaction channels may exist for the generation of QDs. In such channels, on-surface reactions occur between undissolved precursors and dissolved counter precursors (as "ligands") to generate $[CdE]_i$ monomers. In the CdO/OA/Se/ODE reaction system, the surface reaction channels should account for the acceleration of selenium dissolution, and might also promote the dissolution of CdO. In another CdO/OLA/S/ODE reaction system, the surface reaction channel exclusively promoted the conversion of CdO into CdS QDs; OLA and dissolved sulfur as ligands have a synergistic effect on the dissolution of CdO. Such channels may find application in material synthesis via nano-surface reactions.

(iii) In the single-step synthesis, the dissolution of CdO was integrated into the QD growth process. The release of OA during QD formation would in turn promote the dissolution of CdO. The OA circulation should also partly account for the accelerated CdO dissolution in the CdO/OA/S/ODE reaction system.

(iv) The direct use of CdO in the single-step synthesis was able to produce QDs with even better quality than two-step synthesis using preformed cadmium oleate. The pre-dissolution of CdO proves not to be an intrinsic requirement for high-quality synthesis. Single-step synthesis of QDs using CdO and chalcogen has great potential to provide large-scale, cost-effective, yet high-quality synthesis.

4 Experimental

4.1 Chemicals

CdO (99%, Adamas), OA (90%, Aldrich), OLA (70%, Aldrich), TDPA (97%, Aldrich), TOP (90%, Aldrich), ODE (90%, Aldrich), sulfur (99.5%, Chengdu Kelong Chemical), selenium (~ 325 mesh, 99.5% Alfa Aesar), tellurium (~ 325 mesh, 99.99% Alfa Aesar), myristic acid (Tianjin Guangfu Fine Chemical Research Institute), hexane (AR, ≥ 95.0%), and absolute ethanol (AR, ≥ 99.7%) were used as received.

4.2 Single-step syntheses of CdS and CdSe QDs

CdO 0.064 g (0.5 mmol), sulfur powder 0.008 g (0.25 mmol), and oleic acid 1.1 g (3.5 mmol) were mixed with ODE (total 10 g). The mixture, under N_2 flow, was heated to 220 °C (ca. 10 °C/min). The reaction was allowed to proceed at this temperature for 30 min. Aliquots can be taken at different time intervals to follow the reaction. During the heating up process, stirring should be applied carefully to ensure all the solid starting materials were soaked in the solvent. Experimental conditions can be modified to tailor the QD size. Selenium powder 0.02 g (0.25 mmol) was used to replace sulfur for the synthesis of CdSe QDs under otherwise identical conditions.

4.3 Two-step syntheses of CdS and CdSe QDs

At first, 0.064 g of CdO (0.5 mmol), 1.1 g of oleic acid (3.5 mmol), and 8.83 g of ODE were loaded into a 25 mL three-necked flask. The flask, under N_2 flow, was heated to 220 °C and then maintained for 10 min to make a clear solution. The solution was cooled down and was mixed with 8 mg of sulfur powder (0.25 mmol). The mixture, under N_2 flow, was heated to 220 °C (ca. 10 °C/min). The reaction was allowed to proceed at this temperature for 30 min. Aliquots can be taken at different time intervals to follow the reaction. 0.02 g selenium powder (0.025 mmol) was used to prepare CdSe QDs under otherwise same conditions.

4.4 Single-step synthesis of CdTe QDs

0.064 g of CdO (0.5 mmol), 0.032 g of tellurium powder (0.25 mmol), TDPA (1.1 mmol), and TOP (1.1 mmol) were mixed with 9.15 g of ODE. The mixture, under N_2 flow, was

heated to 290 °C (ca. 10 °C/min). The reaction was allowed to proceed at this temperature for 30 min. Aliquots can be taken at different time intervals to follow the reaction. However, a little amount of tellurium was noticed to remain undissolved after the synthesis. Myristic acid and oleic acid (3.5 mmol) were also used to replace TDPA for the synthesis of CdTe nanocrystals at 180 and 200 °C, respectively.

4.5 CdO dissolution experiments

0.064 g of CdO (0.5 mmol), 0.008 g of sulfur powder (0.025 mmol), oleic acid (1.5 mmol), and 9.46 g ODE were loaded in a 25 mL flask. The flask, under N_2 flow, was placed into a hot oil bath at 200 °C. The mixture was stirred (at ca. 1,000 rpm) and heated for 30 min. The reaction flask was withdrawn from the oil bath to observe the dissolution of CdO at an interval of 10 min. For comparison, another experiment without sulfur powder addition was carried out under otherwise identical conditions.

4.6 Selenium dissolution experiments

0.02 g of Se (0.25 mmol), 0.064 g of CdO (0.5 mmol), oleic acid (1.5 mmol), and 9.45 g ODE were loaded in a 25 mL flask. This system was sonicated for 1–2 min. The flask, under N_2 flow, was placed into a hot oil bath at 200 °C. The mixture was stirred (at ca. 1,000 rpm) and heated for 30 min. The reaction flask was withdrawn from the oil bath to observe the dissolution of selenium at an interval of 10 min. For comparison, another experiment without CdO powder addition was carried out under otherwise identical conditions.

4.7 OLA-promoted single-step synthesis of CdS QDs

CdO (0.064 g, 0.5 mmol), sulfur (0.008 g, 0.025 mmol), OLA (1.34 g, 0.35 mmol), and ODE (8.6 g) were loaded in a three-necked flask. Under N_2 flow, the flask was placed in an oil bath already heated to 220 °C. Then the mixture was stirred (at ca. 1,000 rpm) and heated for 20 min. CdO remained largely undissolved. The resulting suspension was centrifuged, and the resulting supernatant and precipitate were used for further characterization. For comparison, the synthesis was also tried in two steps under otherwise same conditions. In the first step, CdO, OLA, and ODE were heated at 220 °C for 20 min. Then the mixture was centrifugated. In the second step, the supernatant was decanted and mixed with sulfur in another flask, which was then heated at 220 °C for 20 min. For further comparison, a mixture of CdO (0.064 g, 0.5 mmol), sulfur (0.008 g, 0.25 mmol), and ODE (9.86 g), without OLA addition, was treated under otherwise identical conditions.

4.8 Characterization

UV–vis absorption spectra of the samples were collected using a UV2310II spectrophotometer (Techcomp, Shanghai). Photoluminescence data were collected using a fluorescence spectrophotometer F-380 (Tianjin Gangdong). For the absorption and photoluminescence measurement, all the samples were diluted in hexane. The TEM images of the quantum dots were taken on a JEOL JEM2100 microscope at 200 kV. PXRD patterns of the samples were recorded on EMPYREAN (with Cu Kα) between 10° and 70°. The PXRD sample was prepared by evaporating drops of concentrated nanocrystal solution in hexane on a glass plate. The samples were purified using hexane/ethanol before TEM and PXRD measurements.

Acknowledgements

This work was supported by the opening project of State Key Laboratory of Polymer Materials Engineering (Sichuan University) (Nos. sklpme2019-4-38 and sklpme2019-4-36). L. X. is grateful to the National Natural Science Foundation of China (NSFC, No. 22005205). Q. Y. sincerely thanks Prof. Kui Yu and her group members for valuable help. Q. Y. also thanks Dr. Chao Chen for valuable help.

Electronic Supplementary Material: Supplementary material (digital pictures of the crude dispersions of CdE QDs after synthesis, optical property, TEM, and PXRD characterizations of the CdE QDs) is available in the online version of this article at https://doi.org/10.1007/s12274-022-5165-x.

References

[1] Efros, A. L.; Brus, L. E. Nanocrystal quantum dots: From discovery to modern development. *ACS Nano* **2021**, *15*, 6192–6210.

[2] De Arquer, F. P. G.; Talapin, D. V.; Klimov, V. I.; Arakawa, Y.; Bayer, M.; Sargent, E. H. Semiconductor quantum dots: Technological progress and future challenges. *Science* **2021**, *373*, eaaz8541.

[3] Mei, W. H.; Zhang, Z. Q.; Zhang, A. D.; Li, D.; Zhang, X. Y.; Wang, H. W.; Chen, Z.; Li, Y. Z.; Li, X. G.; Xu, X. G. High-resolution, full-color quantum dot light-emitting diode display fabricated via photolithography approach. *Nano Res.* **2020**, *13*, 2485–2491.

[4] Jalali, H. B.; Sadeghi, S.; Baylam, I.; Han, M.; Ow-Yang, C. W.; Sennaroglu, A.; Nizamoglu, S. Exciton recycling via InP quantum dot funnels for luminescent solar concentrators. *Nano Res.* **2021**, *14*, 1488–1494.

[5] Zhang, X. S.; Chen, Y. J.; Lian, L. Y.; Zhang, Z. Z.; Liu, Y. X.; Song, L.; Geng, C.; Zhang, J. B.; Xu, S. Stability enhancement of PbS quantum dots by site-selective surface passivation for near-infrared LED application. *Nano Res.* **2021**, *14*, 628–634.

[6] Peng, X. G. An essay on synthetic chemistry of colloidal nanocrystals. *Nano Res.* **2009**, *2*, 425–447.

[7] Murray, C. B.; Norris, D. J.; Bawendi, M. G. Synthesis and characterization of nearly monodisperse CdE (E = sulfur, selenium, tellurium) semiconductor nanocrystallites. *J. Am. Chem. Soc.* **1993**, *115*, 8706–8715.

[8] Peng, Z. A.; Peng, X. G. Formation of high-quality CdTe, CdSe, and CdS nanocrystals using CdO as precursor. *J. Am. Chem. Soc.* **2001**, *123*, 183–184.

[9] Yu, W. W.; Peng, X. G. Formation of high-quality CdS and other II–VI semiconductor nanocrystals in noncoordinating solvents: Tunable reactivity of monomers. *Angew. Chem., Int. Ed.* **2002**, *41*, 2368–2371.

[10] Yu, W. W.; Wang, Y. A.; Peng, X. G. Formation and stability of size-, shape-, and structure-controlled CdTe nanocrystals: Ligand effects on monomers and nanocrystals. *Chem. Mater.* **2003**, *15*, 4300–4308.

[11] Deng, Z. T.; Cao, L.; Tang, F. Q.; Zou, B. S. A new route to zinc-blende CdSe nanocrystals: Mechanism and synthesis. *J. Phys. Chem. B* **2005**, *109*, 16671–16675.

[12] Jasieniak, J.; Bullen, C.; Van Embden, J.; Mulvaney, P. Phosphine-free synthesis of CdSe nanocrystals. *J. Phys. Chem. B* **2005**, *109*, 20665–20668.

[13] Cao, Y. C.; Wang, J. H. One-pot synthesis of high-quality zinc-blende CdS nanocrystals. *J. Am. Chem. Soc.* **2004**, *126*, 14336–14337.

[14] Yang, Y. A.; Wu, H. M.; Williams, K. R.; Cao, Y. C. Synthesis of CdSe and CdTe nanocrystals without precursor injection. *Angew. Chem., Int. Ed.* **2005**, *44*, 6712–6715.

[15] Chen, O.; Chen, X.; Yang, Y. A.; Lynch, J.; Wu, H. M.; Zhuang, J. Q.; Cao, Y. C. Synthesis of metal-selenide nanocrystals using selenium dioxide as the selenium precursor. *Angew. Chem., Int. Ed.* **2008**, *47*, 8638–8641.

[16] Van Embden, J.; Chesman, A. S. R.; Jasieniak, J. J. The heat-up synthesis of colloidal nanocrystals. *Chem. Mater.* **2015**, *27*, 2246–2285.

[17] Steckel, J. S.; Yen, B. K. H.; Oertel, D. C.; Bawendi, M. G. On the mechanism of lead chalcogenide nanocrystal formation. *J. Am. Chem. Soc.* **2006**, *128*, 13032–13033.

[18] Evans, C. M.; Evans, M. E.; Krauss, T. D. Mysteries of TOPSe revealed: Insights into quantum dot nucleation. *J. Am. Chem. Soc.* **2010**, *132*, 10973–10975.
[19] Yu, K.; Liu, X. Y.; Zeng, Q.; Leek, D. M.; Ouyang, J. Y.; Whitmore, K. M.; Ripmeester, J. A.; Tao, Y.; Yang, M. L. Effect of tertiary and secondary phosphines on low-temperature formation of quantum dots. *Angew. Chem., Int. Ed.* **2013**, *52*, 4823–4828.
[20] Yu, K.; Liu, X. Y.; Zeng, Q.; Yang, M. L.; Ouyang, J. Y.; Wang, X. Q.; Tao, Y. The formation mechanism of binary semiconductor nanomaterials: Shared by single-source and dual-source precursor approaches. *Angew. Chem., Int. Ed.* **2013**, *52*, 11034–11039.
[21] Yu, K.; Liu, X. Y.; Qi, T.; Yang, H. Q.; Whitfield, D. M.; Y Chen, Q.; Huisman, E. J. C.; Hu, C. W. General low-temperature reaction pathway from precursors to monomers before nucleation of compound semiconductor nanocrystals. *Nat. Commun.* **2016**, *7*, 12223.
[22] Lai, R. C.; Pu, C. D.; Peng, X. G. On-surface reactions in the growth of high-quality CdSe nanocrystals in nonpolar solutions. *J. Am. Chem. Soc.* **2018**, *140*, 9174–9183.
[23] Zhu, C. Q.; Chen, D. D.; Cao, W. C.; Lai, R. C.; Pu, C. D.; Li, J. Z.; Kong, X. Q.; Peng, X. G. Facet-dependent on-surface reactions in the growth of CdSe nanoplatelets. *Angew. Chem., Int. Ed.* **2019**, *58*, 17764–17770.
[24] Abécassis, B.; Bouet, C.; Garnero, C.; Constantin, D.; Lequeux, N.; Ithurria, S.; Dubertret, B.; Pauw, B. R.; Pontoni, D. Real-time *in situ* probing of high-temperature quantum dots solution synthesis. *Nano Lett.* **2015**, *15*, 2620–2626.
[25] Li, J. Z.; Wang, H. F.; Lin, L.; Fang, Q.; Peng, X. G. Quantitative identification of basic growth channels for formation of monodisperse nanocrystals. *J. Am. Chem. Soc.* **2018**, *140*, 5474–5484.
[26] Zhang, J.; Hao, X. Y.; Rowell, N.; Kreouzis, T.; Han, S.; Fan, H. S.; Zhang, C. C.; Hu, C. W.; Zhang, M.; Yu, K. Individual pathways in the formation of magic-size clusters and conventional quantum dots. *J. Phys. Chem. Lett.* **2018**, *9*, 3660–3666.
[27] Li, L. J.; Zhang, J.; Zhang, M.; Rowell, N.; Zhang, C. C.; Wang, S. L.; Lu, J.; Fan, H. S.; Huang, W.; Chen, X. Q. et al. Fragmentation of magic-size cluster precursor compounds into ultrasmall CdS quantum dots with enhanced particle yield at low temperatures. *Angew. Chem., Int. Ed.* **2020**, *59*, 12013–12021.
[28] Li, Y.; Rowell, N.; Luan, C. R.; Zhang, M.; Chen, X. Q.; Yu, K. A two-pathway model for the evolution of colloidal compound semiconductor quantum dots and magic-size clusters. *Adv. Mater.*, in press, https://doi.org/10.1002/adma.202107940.
[29] Shen, J.; Luan, C. R.; Rowell, N.; Li, Y.; Zhang, M.; Chen, X. Q.; Yu, K. Size matters: Steric hindrance of precursor molecules controlling the evolution of CdSe magic-size clusters and quantum dots. *Nano Res.* **2022**, *15*, 8664–8572.
[30] Zhang, W. J.; Jin, C.; Yang, Y. J.; Zhong, X. H. Noninjection facile synthesis of gram-scale highly luminescent CdSe multipod nanocrystals. *Inorg. Chem.* **2012**, *51*, 531–535.
[31] Zhang, W. J.; Zhang, H.; Feng, Y. Y.; Zhong, X. H. Scalable single-step noninjection synthesis of high-quality core/shell quantum dots with emission tunable from violet to near infrared. *ACS Nano* **2012**, *6*, 11066–11073.
[32] Zhang, W. J.; Zhang, H.; Zhong, X. H. Noninjection ultralarge-scaled synthesis of shape-tunable CdS nanocrystals as photocatalysts. *RSC Adv.* **2013**, *3*, 17477–17484.
[33] Yordanov, G. G.; Yoshimura, H.; Dushkin, C. D. Phosphine-free synthesis of metal chalcogenide quantum dots by means of *in situ*-generated hydrogen chalcogenides. *Colloid Polym. Sci.* **2008**, *286*, 813–817.
[34] Talapin, D. V.; Haubold, S.; Rogach, A. L.; Kornowski, A.; Haase, M.; Weller, H. A novel organometallic synthesis of highly luminescent CdTe nanocrystals. *J. Phys. Chem. B* **2001**, *105*, 2260–2263.
[35] Lu, W. G.; Fang, J. Y.; Stokes, K. L.; Lin, J. Shape evolution and self assembly of monodisperse PbTe nanocrystals. *J. Am. Chem. Soc.* **2004**, *126*, 11798–11799.
[36] Sun, H. C.; Wang, F. D.; Buhro, W. E. Tellurium precursor for nanocrystal synthesis: Tris(dimethylamino)phosphine telluride. *ACS Nano* **2018**, *12*, 12393–12400.
[37] Pu, C. D.; Zhou, J. H.; Lai, R. C.; Niu, Y.; Nan, W. N.; Peng, X. G. Highly reactive, flexible yet green Se precursor for metal selenide nanocrystals: Se–octadecene suspension (Se–SUS). *Nano Res.* **2013**, *6*, 652–670.
[38] Flamee, S.; Cirillo, M.; Abe, S.; De Nolf, K.; Gomes, R.; Aubert, T.; Hens, Z. Fast, high yield, and high solid loading synthesis of metal selenide nanocrystals. *Chem. Mater.* **2013**, *25*, 2476–2483.
[39] Hu, X. F.; Li, J. Z.; Wang, Z.; Qian, X. D.; Zhu, C. Q.; Peng, X. G. Universal precursors dispersed in vaseline–octadecene gel for nanocrystal synthesis. *Nano Res.* **2022**, *15*, 4724–4731.
[40] Wang, L.; Wang, J.; Chen, Y.; Zhong, H. H.; Jiang, Y. One-pot synthesis of CdS quantum dots and their quantum yields. *Chem. J. Chin. Univ.* **2011**, *32*, 1043–1048.
[41] Li, Z.; Ji, Y. J.; Xie, R. G.; Grisham, S. Y.; Peng, X. G. Correlation of CdS nanocrystal formation with elemental sulfur activation and its implication in synthetic development. *J. Am. Chem. Soc.* **2011**, *133*, 17248–17256.
[42] García-Rodríguez, R.; Hendricks, M. P.; Cossairt, B. M.; Liu, H. T.; Owen, J. S. Conversion reactions of cadmium chalcogenide nanocrystal precursors. *Chem. Mater.* **2013**, *25*, 1233–1249.
[43] Bullen, C.; Van Embden, J.; Jasieniak, J.; Cosgriff, J. E.; Mulder, R. J.; Rizzardo, E.; Gu, M.; Raston, C. L. High activity phosphine-free selenium precursor solution for semiconductor nanocrystal growth. *Chem. Mater.* **2010**, *22*, 4135–4143.
[44] Furrer, G.; Stumm, W. The coordination chemistry of weathering: I. Dissolution kinetics of δ-Al_2O_3 and BeO. *Geochim. Cosmochim. Ac.* **1986**, *50*, 1847–1860.
[45] Zinder, B.; Furrer, G.; Stumm, W. The coordination chemistry of weathering: II. Dissolution of Fe(III) oxides. *Geochim. Cosmochim. Ac.* **1986**, *50*, 1861–1869.
[46] Stumm, W.; Wollast, R. Coordination chemistry of weathering: Kinetics of the surface-controlled dissolution of oxide minerals. *Rev. Geophys.* **1990**, *28*, 53–69.
[47] Lin, S. X.; Li, J. Z.; Pu, C. D.; Lei, H. R.; Zhu, M. Y.; Qin, H. Y.; Peng, X. G. Surface and intrinsic contributions to extinction properties of ZnSe quantum dots. *Nano Res.* **2020**, *13*, 824–831.
[48] Yu, K. CdSe magic-sized nuclei, magic-sized nanoclusters and regular nanocrystals: Monomer effects on nucleation and growth. *Adv. Mater.* **2012**, *24*, 1123–1132.
[49] Su, M. Y.; Li, X. Y.; Zhang, J. T. Telluride semiconductor nanocrystals: Progress on their liquid-phase synthesis and applications. *Rare Met.* **2022**, *41*, 2527–2551.
[50] Son, D. H.; Hughes, S. M.; Yin, Y. D.; Alivisatos, A. P. Cation exchange reactions in ionic nanocrystals. *Science* **2004**, *306*, 1009–1012.
[51] McCarthy, C. L.; Webber, D. H.; Schueller, E. C.; Brutchey, R. L. Solution-phase conversion of bulk metal oxides to metal chalcogenides using a simple thiol-amine solvent mixture. *Angew. Chem., Int. Ed.* **2015**, *54*, 8378–8381.
[52] Tian, Q. W.; Cui, Y.; Wang, G.; Pan, D. C. A robust and low-cost strategy to prepare Cu_2ZnSnS_4 precursor solution and its application in $Cu_2ZnSn(S,Se)_4$ solar cells. *RSC Adv.* **2015**, *5*, 4184–4190.
[53] Shinato, K. W.; Huang, F. F.; Xue, Y. P.; Wen, L.; Jin, Y.; Mao, Y. J.; Luo, Y. Synergistic inhibitive effect of cysteine and iodide ions on corrosion behavior of copper in acidic sulfate solution. *Rare Met.* **2021**, *40*, 1317–1328.
[54] Zhu, R. L.; Li, X. B.; Wei, C.; Huang, H.; Li, M. T.; Li, C. X.; Tang, F. L. Synergistic extraction of zinc from ammoniacal solutions using a β-diketone mixed with trialkylphosphine oxide. *Rare Met.* **2019**, *38*, 270–276.
[55] Chan, E. M.; Xu, C. X.; Mao, A. W.; Han, G.; Owen, J. S.; Cohen, B. E.; Milliron, D. J. Reproducible, high-throughput synthesis of colloidal nanocrystals for optimization in multidimensional parameter space. *Nano Lett.* **2010**, *10*, 1874–1885.
[56] Ouyang, J. Y.; Zaman, M. B.; Yan, F. J.; Johnston, D.; Li, G.; Wu, X. H.; Leek, D.; Ratcliffe, C. I.; Ripmeester, J. A.; Yu, K. Multiple families of magic-sized CdSe nanocrystals with strong bandgap photoluminescence via noninjection one-pot syntheses. *J. Phys.*

Chem. C **2008**, *112*, 13805–13811.
[57] Houtepen, A. J.; Koole, R.; Vanmaekelbergh, D.; Meeldijk, J.; Hickey, S. G. The hidden role of acetate in the PbSe nanocrystal synthesis. *J. Am. Chem. Soc.* **2006**, *128*, 6792–6793.
[58] Narayanaswamy, A.; Xu, H. F.; Pradhan, N.; Kim, M.; Peng, X. G. Formation of nearly monodisperse In_2O_3 nanodots and oriented-attached nanoflowers: Hydrolysis and alcoholysis vs. pyrolysis. *J. Am. Chem. Soc.* **2006**, *128*, 10310–10319.
[59] Zhang, H. T.; Savitzky, B. H.; Yang, J.; Newman, J. T.; Perez, K. A.; Hyun, B. R.; Kourkoutis, L. F.; Hanrath, T.; Wise, F. W. Colloidal synthesis of PbS and PbS/CdS nanosheets using acetate-free precursors. *Chem. Mater.* **2016**, *28*, 127–134.
[60] Ithurria, S.; Dubertret, B. Quasi 2D colloidal CdSe platelets with thicknesses controlled at the atomic level. *J. Am. Chem. Soc.* **2008**, *130*, 16504–16505.
[61] Li, Z.; Qin, H. Y.; Guzun, D.; Benamara, M.; Salamo, G.; Peng, X. G. Uniform thickness and colloidal-stable CdS quantum disks with tunable thickness: Synthesis and properties. *Nano Res.* **2012**, *5*, 337–351.
[62] Yu, W. W.; Qu, L. H.; Guo, W. Z.; Peng, X. G. Experimental determination of the extinction coefficient of CdTe, CdSe, and CdS nanocrystals. *Chem. Mater.* **2003**, *15*, 2854–2860.
[63] Abe, S.; Capek, R. K.; De Geyter, B.; Hens, Z. Reaction chemistry/nanocrystal property relations in the hot injection synthesis, the role of the solute solubility. *ACS Nano* **2013**, *7*, 943–949.
[64] Hendricks, M. P.; Campos, M. P.; Cleveland, G. T.; Jen-La Plante, I.; Owen, J. S. A tunable library of substituted thiourea precursors to metal sulfide nanocrystals. *Science* **2015**, *348*, 1226–1230.
[65] Campos, M. P.; Hendricks, M. P.; Beecher, A. N.; Walravens, W.; Swain, R. A.; Cleveland, G. T.; Hens, Z.; Sfeir, M. Y.; Owen, J. S. A library of selenourea precursors to PbSe nanocrystals with size distributions near the homogeneous limit. *J. Am. Chem. Soc.* **2017**, *139*, 2296–2305.